PHYSICAL REVIEW B, VOLUME 63, 085308

Au/GaN interface: Initial stages of formation and temperature-induced effects

A. Barinov, L. Casalis, L. Gregoratti, and M. Kiskinova
Sincrotrone Trieste, Area Science Park, 34012 Trieste, Italy
(Received 28 June 2000; revised manuscript received 10 October 2000; published 1 February 2001)

Synchrotron radiation photoemission spectromicroscopy has been used to study the properties of an Au/GaN interface starting from an atomically clean GaN surface. The effects of Au coverage and temperature were examined. The results have demonstrated that annealing alters the height of the Schottky barrier, formed after deposition of a 4-monolayer (ML) Au film at room temperature. The photoemission spectra indicate that these barrier changes should be attributed to structural rearrangements of the Au film and to formation of a Au gallide interfacial layer, a product of the reaction between the Au and GaN above 500 °C. The photoemission images have revealed that spatial heterogeneity in the composition is developed at temperatures above 750 °C. The large spread of the Au/GaN barrier heights reported in the literature was discussed considering the current theoretical concepts.

DOI: 10.1103/PhysRevB.63.085308 PACS number(s): 73.30.+y, 82.65.+r, 68.35.−p

I. INTRODUCTION

Growth of a sufficiently high-quality material and subsequent formation of stable metal contacts are the main challenges of GaN-based device technology.[1–4] At elevated temperatures the onset of metal-GaN reactions can change the interface chemistry and morphology dramatically, a general concern in high-temperature electronics. However, many aspects of contact formation, such as the development of surface band bending with metal coverage, the nature of metal/GaN interactions, and the temperature-induced effects are still not well understood.[2,4] There is a large spread of Schottky barrier height (SBH) values reported in the literature for the same metal/n-type GaN system. This is certainly related to the different conditions of the GaN surfaces before metal deposition, namely, structural quality and cleanliness. Defects introduced during the growth of GaN epilayers on lattice-mismatched substrates can lead to lateral variations in the SBH, whereas contaminated surfaces can affect carrier transport through the contact. Still it is not clear how the changes in interface morphology and chemistry, which occur at elevated temperatures, affect the electric properties of the contact.

Many controversial results have been reported for interaction of Au films with GaN, the most extensively studied metal/GaN Schottky contact. Nonreactive layer-by-layer growth up to ~10 ML at room temperature and formation of Au islands after annealing to 600 °C was reported in Ref. 5, whereas formation of an alloy layer with unspecified composition was suggested for explaining the different performance of Au/GaN contacts fabricated at room and low temperatures.[6] According to the most recent ballistic-electron-emission-microscopy (BEEM) study the Au/GaN SBH can be substantially altered by preannealing of the GaN before Au deposition, due to vacancy diffusion.[7] The BEEM results have also revealed lateral nonuniformity of SBH at length scales larger than 0.1 μm. The dispersion of the Au/n-type GaN SBH experimental values is also quite significant, they vary between ~1.0 and 1.4 eV.[2,4–8] The theoretically calculated value for an ideal Au/GaN interface is 1.08 eV, which fortuitously coincides with the value measured by BEEM.[9]

The present investigation is focused on two issues: the initial stage of Au/n-type GaN interface formation starting from an atomically clean GaN surface and the temperature-induced morphological and chemical changes. Employing synchrotron radiation, photoelectron spectromicroscopy has allowed us to obtain information from submicrometer interface areas and to examine the effect of spatial chemical heterogeneity, developed at elevated temperature, on the interface electronic structure.

II. EXPERIMENT

The experiments were carried out with the scanning photoelectron microscope (SPEM) at the ELETTRA synchrotron light source.[10] The SPEM uses zone plate optics for producing a microprobe with submicrometer dimensions, in this experiment with a diameter of 0.12 μm. The emitted photoelectrons from this microspot are collected by a hemispherical electron energy analyzer set at an angle of 70° with respect to the sample normal. This geometry of the normal-incidence beam and very grazing acceptance angle gives a very high sensitivity to the surface. The effective escape depths for the N 1s, Au 4f, and Ga 3d photoelectrons was ~2.6, 3.4, and 3.6 Å, respectively, for the photon energy of 495 eV. To obtain two-dimensional chemical maps the electron analyzer is set to collect photoelectrons within a selected kinetic energy window while the sample position is scanned with respect to the focused beam. The use of a 16-channel detector allows acquiring 16 images with a single scan. Each image corresponds to a specific kinetic energy, defined by the covered energy window at which the analyzer is set. The 16-channel imaging can be used not only for comparing the contrast but also for reconstructing part or all of the spectrum corresponding to the energy window.[11] The microspectroscopy mode is in fact measuring photoelectron spectra from a selected microspot on the sample. The measurement station is also equipped with facilities for sample preparation, metal evaporation, and characterization of the surface structure and cleanliness with low-energy electron diffraction (LEED) and

 ©2001 The American Physical Society

Auger electron spectroscopy (AES). During metal evaporation, thermal treatments, and SPEM measurements the pressure in the UHV chambers was kept in the low-10^{-10}-mbar range.

In order to avoid the problem of charging when applying photoelectron spectroscopy wurtzite-GaN(0001) films grown by molecular beam epitaxy (MBE) on Si(111) substrates were used. The growth of GaN films on Si substrates is desirable for accomplishment the integration with Si electronics, but, because of the larger lattice misfit, the GaN epilayer contains a larger number of defects than GaN grown on sapphire.[3] The samples were naturally n-doped through N vacancies ($n \sim 10^{17}\,\mathrm{cm}^{-3}$). They were mounted to the sample holder through Ta clips and were resistively heated. The temperatures above 250 °C were measured using a pyrometer. Atomically clean GaN surfaces were obtained employing the same procedure adopted for metal-organic chemical vapor deposition (MOCVD) GaN films grown on a sapphire substrate: cycles of N_2 ion sputtering and annealing to 900 °C.[8,12] The LEED pattern after this cleaning procedure was a facetted (1×1) structure with very faint (3×3) extra spots. It was almost identical to the pattern reported for an atomically clean n-type GaN grown on sapphire.[12] According to the structural models this surface can be described as N-terminated GaN with a (1×1)Ga adlayer and a few (3×3) domains formed by Ga adatoms.[13]

Au was deposited at room temperature through a $1.0\times0.064\text{-mm}^2$ mask at a low rate of ~0.08 ML/min in the order to suppress clustering during the film growth. 1 ML equals the atomic density of an ideal GaN(0001) surface, $1.14\times10^{15}\,\mathrm{atoms\,cm}^{-2}$. Using a SPEM we can measure the Au $4f$, Ga $3d$, and N $1s$ maps and the photoelectron spectra inside and across the edge of the Au patch. Figure 1(a) shows an Au $4f_{7/2}$ map, centered to the edge of a 4-ML Au patch deposited at room temperature. The part covered with Au appears bright and homogeneous at our length scale of 0.12 μm. The sharpness of the patch edge depends on the distance between the mask and the sample and provides a natural gradient in the amount of deposited metal. In the present experiment this area is about 10–15 μm wide and allows precise monitoring the interface evolution with increasing Au coverage from 0 to 4 ML. As will be shown below the changes in the morphology of the interface induced by annealing result in lateral variations in the gray level of the Au $4f$, Ga $3d$, and N $1s$ maps inside the patch. Another advantage of the patch is that the state of the Au-free GaN surface can be checked under the same experimental conditions as a reference.

The photoelectron spectra were fitted with the minimum number of components, using Gaussian-Lorenzian curves with Doniach-Sunjic asymmetry for metallic phases. The energy resolution of 0.3 eV allowed accuracy better than 0.1 eV in determination of the peak shifts. The position of the equilibrium Fermi level, E_F, was measured from the Fermi edge developed inside the 4-ML Au patch, which coincided with the Fermi edge measured on the Ta clips holding the sample.

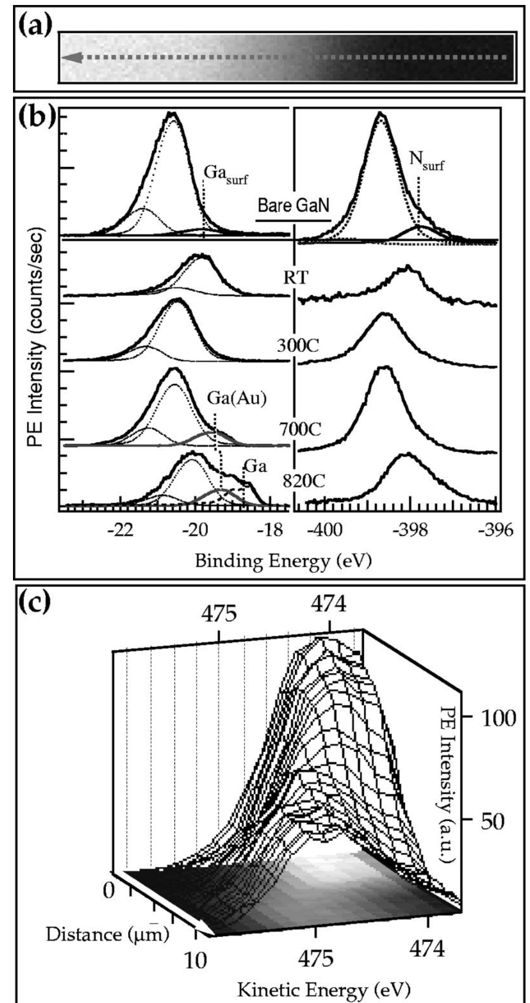

FIG. 1. (a) Au $4f_{7/2}$ map centered to the edge of a 4-ML Au patch, deposited at room temperature. (b) Ga $3d$ and N $1s$ spectra measured inside the 4-ML Au patch before and after annealing to different temperatures. The top panel shows the Ga $3d$ and N $1s$ spectra from an Au-free GaN surface. The components attributed to Au gallide, Ga(Au), and metallic Ga,Ga, are drawn with full and dashed lines, respectively. Dotted lines are used for the ''bulk'' GaN components. (b) Intensity-energy-position surface map of Ga $3d$ photoemission across the edge of the Au patch measured at room temperature. The lowest and the highest Ga $3d$ intensities correspond to spots inside and outside the Au patch, respectively. The arrows in (a) and (c) indicate the direction towards the patch.

III. RESULTS

A. GaN surface

The photoemission spectra from a freshly cleaned GaN sample proved that the surface was free of contaminants. The valence-band maximum (VBM) of this surface appeared at 2.8 ± 0.1 eV below the equilibrium E_F, indicating about 0.50 eV upward band bending. This bare surface barrier height (BSBH) is lower than the values reported previously for UHV prepared n-type GaN surfaces (0.75–2.2 eV).[5,8,12] We suppose that this is caused by the presence of surface photovoltage (SPV) in our case, which leads to band flattening.[14] The SPV is one of the undesirable effects of the high flux

density ($\geqslant 10^{11}$ photons s^{-1} μm^{-2}), required by photoelectron microscopy.[10,15] By varying the sample temperature we measured in a separate SPEM experiment that the SPV value for our GaN samples was about 0.2 ± 0.1 eV. As will be demonstrated below this ''undesired'' SPV effect can be used as an indicator for changes in the Au film conductivity induced by structural rearrangements or chemical reactions.

The Ga 3d and N 1s spectra taken on the Au-free GaN surface are shown in Fig. 1(b). The Ga 3d peak is almost identical with the Ga 3d spectra reported by other authors.[8,12,16,17] It is broad and asymmetric with a maximum at 17.7 eV below the VBM. The Ga 3d peak requires three fitting components, a dominant component, which determines the Ga 3d maximum, and two weak components fitting the higher- and lower-binding-energy sides of the Ga 3d spectra. Only the lower-binding-energy component is removed by adsorption of Au and we assign it as a ''surface'' component. The N 1s spectra require a more pronounced ''surface'' component, which is consistent with the smaller escape depth of the N 1s photoelectrons.

B. Au on GaN at room temperature

Figure 1(b) shows that the Ga 3d and N 1s spectra taken inside the 4-ML Au patch after Au deposition at room temperature have lower intensity and are shifted to a lower binding energy. The Ga 3d and N 1s spectra taken in microspots across the patch edge showed gradual attenuation in intensity and continuous energy shift with increasing Au coverage. Figure 1(c) shows a surface plot of the Ga 3d region derived from a 16-channel Ga 3d image centered at the Au patch edge. In this plot the changes of the Ga 3d energy and intensity as a function of Au coverage are visualized. As will be discussed below the observed energy shift is a combined effect of band bending and a decrease of the SPV-induced band flattening. A notable feature was that the rate of attenuation of Ga 3d and N 1s intensities deviated from the expected for a layerwise growth mode when the deposited Au amount exceeded ~1.5 ML.

Figure 2(a) shows a selected set of Au 4f spectra taken in spots inside and across the patch edge and the corresponding photoelectron emission around the Fermi edge. The Au 4f spectra reveal that the natural intensity gain with increasing Au coverage is accompanied by substantial changes in the line shape and peak position. At Au coverage less than 1 ML the Au 4f spectra need two fitting components, assigned as I-Au1 and I-Au2. The binding energy of these components is by 0.9 eV (I-Au1) and 0.3 eV (I-Au2) higher than the Au 4f binding energy of metallic Au (Au $4f_{7/2}$=84.0 eV). Both components appear simultaneously with the first doses of Au and we attribute them to Au atoms from the interfacial layer, which are in contact with the GaN surface. The weak I-Au1 component most likely represents Au atoms adsorbed at defect sites. The I-Au1 grows to about 1 ML and its contribution becomes negligible at high coverage. The main interface component, I-Au2, grows continuously up to about 3.5 ML. The I-Au components follow the same energy shifts with increasing Au coverage as the Ga 3d and N 1s peaks. Above 1 ML a third component, M-Au, emerges and grows in parallel with the I-Au2 component. The Au $4f_{7/2}$ binding energy of the M-Au is 84.0 eV and corresponds to that of metallic Au. Notable features in the evolution of the Au 4f spectra are the slow saturation of the I-Au2 component (far above 1 ML) and the slow increase of the M-Au intensity with an increase of the amount of deposited Au, compared to the rate expected for a layer-by-layer growth mode. The insert in Fig. 2(a) shows the appearance of a Fermi-level emission at Au coverage >1.0 ML, which reflects an increasingly metallic nature of the Au film with increasing Au coverage. The Fermi edge, which appears at ~0.5 eV below the equilibrium E_F position, sharpens with increasing Au coverage. The reduction in SPV occurs between 3 and 4 ML when the E_F emission reaches its equilibrium position.

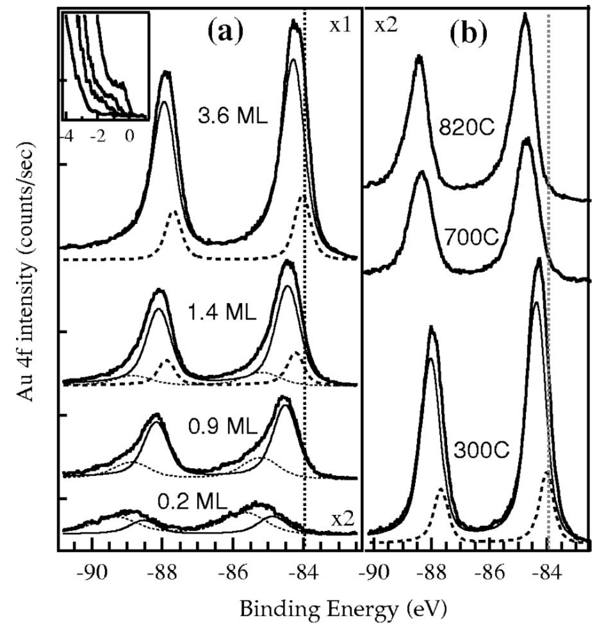

FIG. 2. (a) Evolution of the Au 4f spectra as a function of Au coverage, measured in spots across the patch edge. The insert shows the corresponding emission close to the Fermi edge. The fitting components, I-Au1, I-Au2, and M-Au, are drawn with dotted, full, and dashed lines, respectively. The equilibrium energy position of the M-Au component, 84.0 eV is also indicated. (b) Au 4f spectra measured inside the 4-ML Au patch after annealing to different temperatures. In order to outline the chemical shifts related to formation of Au gallides the energy positions of the spectra in (b) are corrected for SPV.

The SBH value evaluated from the present photoemission results for Au coverage of 4 ML, is 1.4 ± 0.1 eV. By correcting for the SPV effect, it has been found that this value is reached at about 1.4 ML, i.e., when the Fermi emission becomes distinctive.

C. Evolution of the Au/GaN interface at elevated temperatures

The temperature-induced effects on the structure and composition of the 4-ML Au/GaN interface are manifested by the spectra measured inside the Au patch and shown in Figs. 1(b) and 2(b). A general trend, observed with increasing annealing temperature up to 750 °C, is an increase of the

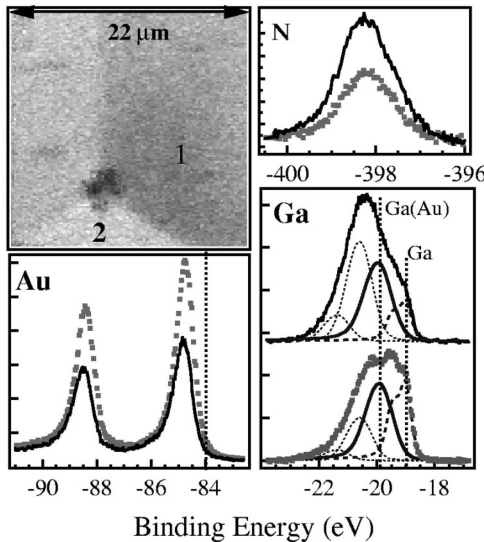

FIG. 3. Au $4f_{7/2}$ image, measured inside the Au patch after annealing to 820 °C, and the Au $4f$ N $1s$, and Ga $3d$ spectra measured in spots 1 (full lines) and 2 (dotted lines).

Ga $3d$ and N $1s$ intensities and attenuation of the Au $4f$ signal. However, there is a distinct difference in the temperature-induced effects on the line shape of the spectra for temperatures below and above 500 °C.

The results obtained after annealing up to 300 °C [see Figs. 1(b) and 2(b)] reveal that the Ga $3d$, N $1s$, and Au $4f$ spectra undergo only intensity changes, accompanied by a shift of the entire photoemission spectrum to a higher binding energy partly due to reappearance of the SPV. This energy shift indicates that the continuity of the Au film is broken. The observed changes after annealing below 500 °C are apparently induced by structural rearrangements of the Au film, because, as will be shown below, the onset of a chemical reaction between Au and GaN leads to distinct line-shape changes of the Ga $3d$, N $1s$, and Au $4f$ spectra.

The photoelectron spectra show evidence of chemical interactions between the Au film and GaN above 500 °C. As can be seen in Fig. 1(b) annealing up to ~750 °C leads to growth of the first reaction-related component in the Ga $3d$ spectrum, Ga(Au). The Ga(Au) component is shifted to a lower binding energy by ~0.8 eV with respect to the dominant Ga $3d$ peak of GaN. Annealing temperatures above 750 °C lead to growth of the second reaction-related component in the Ga $3d$ spectra with a binding energy identical to metallic Ga. We attribute the Ga(Au) component to formation of an Au-gallide interfacial layer. This is in accordance with the observed elimination of the M-Au component and shifts of the Au $4f$ lines to a higher binding energy [Fig. 2(b)]. This temperature-induced degradation of the Au/GaN interface is accompanied by removal of the SPV, indicating that a continuous metallic (Ga and/or Au-Ga alloy) film is formed.

Another very important temperature effect is the reaction-induced lateral inhomogeneity in the interface composition, clearly observed after annealing above 750 °C. Figure 3 shows the Au $4f$ map of an area inside the Au patch, developed after annealing at 820 °C. The contrast of the image

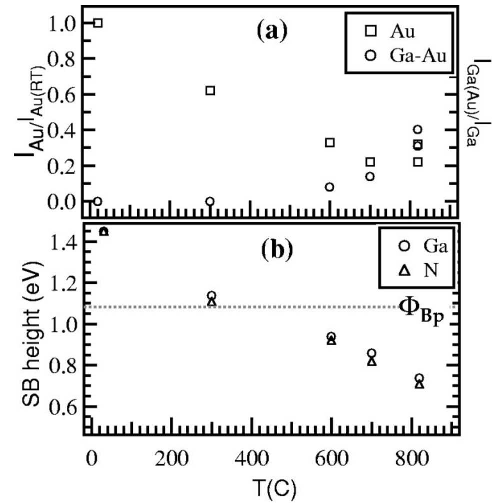

FIG. 4. (a) Changes in the intensity of the Au $4f$ spectra and of the gallide component, Ga(Au), in the Ga $3d$ spectra as a function of annealing temperature. The Au $4f$ signal is normalized against the Au $4f$ intensity measured at room temperature. The Ga(Au) signal is normalized against the total intensity of the corresponding Ga $3d$ peak. The two points at 820 °C define the intensity variations of the Au and Ga(Au) signals due to the developed composition heterogeneity. (b) Barrier height, Φ_{Bn}, as a function of annealing temperature, evaluated from the energy shifts of Ga $3d$ and N $1s$ lines and corrected for SPV. All results refer to measurements inside the 4-ML Au patch. The dashed line indicates the theoretical Φ_{Bn} value for an ''ideal'' Au/GaN contact (Ref. 9).

reveals that the selected area consists of three grains with different Au content. We tentatively relate the grains to the defective GaN microstructure. The dark spot between the grains is a topographic defect, probably holes caused by the released nitrogen.[18] The different composition of the metallic films covering the grains is confirmed by the corresponding Ga $3d$ and Au $4f$ spectra. The fit of the Ga $3d$ spectra taken inside the two different grains shows that the amount of metallic Ga is larger on the grain containing more Au. The corresponding intensity of the N $1s$ spectra from the GaN substrate below indicates different thickness of the Au gallide and Ga films as well. Apparently the Au-GaN interfacial reaction has advanced to different extents, which indicates a different local reactivity of the grains. The induced heterogeneity suggests a mass transport of Au to the more reactive areas. This is in accordance with the enhanced Au mobility observed above 750 °C, which also led to substantial broadening of the Au profiles across the edge.[19] A distinct feature of the spectra shown in Fig. 4 is the identical energy position of the N $1s$ lines. The measured positions of the Fermi edge also were identical and coincided with the equilibrium one.

After annealing to 870 °C we observed complete degradation of the Au/GaN interface and formation of Au-Ga islands with dimensions from sub-μm to a few μm.[19] Reference measurements of the areas outside the patch did not show any degradation of the Au-free GaN up to 900 °C. This confirms that all observed processes are related to the presence of Au.

IV. DISCUSSION

Figure 4 shows two panels with plots that illustrate the temperature-induced changes in the Au/GaN interface structure and the corresponding changes in the Schottky barrier height. The dashed line indicates the SBH value for a nonreactive N-terminated ordered GaN/Au interface, $\Phi_{Bn} = 1.08$ eV, obtained by *ab initio* local-density fully linearized augmented plane-wave (FLAPW) calculations.[9] A very similar SBH value, $\Phi_{Bn} = 1.12$ eV, can also be obtained using the relationship given by the simplistic metal-induced gap states (MIGS) model:[20]

$$\Phi_{Bn} = \Phi_{bp} + S_x(\chi_{\mathrm{Au}} - \chi_{\mathrm{GaN}}), \tag{1}$$

where the theoretically evaluated value for the zero-charge-transfer barrier height, Φ_{bp}, is 1.05 eV,[21] the slope parameter S_x, derived from the relation $A/S - 1 \approx 0.1(\varepsilon_\infty - 1)^2$ $[\varepsilon_\infty(\mathrm{GaN}) \approx 5.35]$,[22] is 0.6, and the Pauling electronegativities are $\chi_{\mathrm{Au}} = 2.54$ and $\chi_{\mathrm{GaN}} = 2.42$.

The measured Schottky barrier height for our 4-ML Au film deposited at room temperature is in agreement only with the value reported in the photoemission studies of Wu and Kahn.[8] It is higher by 0.3 eV than the theoretically predicted value. It also is by 0.2–0.4 eV higher than the barrier heights reported in the literature, measured using different methods (I-V, C-V, BEEM).[2,4–7] These differences are most likely caused by the different surface preparation prior to metal growth. Our AES and photoemission measurements showed that the procedures used in Refs. 4–7, *ex situ* chemical treatment and annealing in inert gas or UHV, are effective in removing part of the oxide and other contaminants but cannot produce an atomically clean surface. Here we deposited Au on an atomically clean, N-terminated GaN, covered with a Ga adlayer. Our GaN surface was far from the ideal case of the N-terminated GaN, used in the *ab initio* calculations,[9] or an initial semiconductor surface with flat bands.[23] For example, the presence of acceptor surface states on the initial surface will lead to a Φ_{bp} value in Eq. (1) higher than the theoretically estimated one. The lack of Fermi-level pinning in GaN case, suggested in Ref. 9, undoubtedly may also contribute to the large spread of the SBH values. Finally, it should be noted that due to the high surface sensitivity we probe the highest barrier height.[24] However, the object of the present study is not to measure the absolute values of the SBH but to examine the initial stages of formation of the Au/n-type GaN(0001) interface and the temperature-induced changes in interfacial properties and homogeneity.

Let us first discuss the results obtained at temperatures below the onset of a chemical reaction. The evolution of the Au/GaN interface at room temperature has revealed that the changes in the intensity of the Au $4f$, Ga $3d$ and N $1s$ spectra with increasing deposited Au amount does not confirm the layer-by-layer growth mode, suggested in Ref. 5. The deviation becomes obvious when the Au amount exceeds about 1.5 ML. It is well known that layerwise growth behavior can also result from the formation of small islands[25] When the density of these islands increases to an extent that the adjacent islands touch the thickness of the layer is not far from 1 ML. Such metal films, being in a thermodynamically nonequilibrium state, agglomerate into larger islands at elevated temperature uncovering parts of the substrate surface. In photoemission experiments this structural rearrangement leads to attenuation of the signal from the metal film and an increase of the signal from the substrate. This is what we observed in the present case when the 4-ML Au film was annealed to 300 °C. The break of the continuity of the film due to these changes in the film morphology naturally leads to the observed reappearance of SPV. In addition to the agglomeration other process that is likely to take place at the interface concerns the presence of a Ga adlayer on our initial GaN surface. At elevated temperature an atomic exchange between the Au film and the Ga adlayer is possible. These structural rearrangements after annealing to 300 °C affect the SBH [see Fig. 4(b)]. Removal of residual surface states or changes in the bonding of the Au atoms to the surface are two possible reasons for the SBH reduction. As discussed in Ref. 9, the poor screening properties of GaN increase the role of the electric dipole layer, i.e., appreciable SBH variations can be induced by structural effects. Apparently the reported different performance of contacts fabricated at liquid-nitrogen and room temperatures[6] may be attributed to structural differences between the formed Au interfacial layers. Another possible process, penetration of Au atoms inside the ''nanopipes'' (a characteristic defect of the GaN material[1]) will lead only to reduction of the Au $4f$ signal, but should not affect the SBH.

According to the Au-Ga solid-solution diagram Au gallide phases are already formed at temperatures above 270 °C.[26] The higher temperature (above 500 °C), required in the present system, can be explained with the activation energy barrier of the Au-GaN reaction, which involves penetration of Au inside the GaN lattice and disruption of the top GaN layers. The evolution of the Au $4f$ and Ga $3d$ spectra indicate that the stoichiometry of the formed Au-gallide alloy changes, becoming Ga-rich with increasing temperature. The Ga(Au)/Au atomic ratio, evaluated taking into account the Ga $3d$ and Au $4f$ cross sections, reaches 1.8 ± 0.2 after annealing to 820 °C. This value is close to the stoichiometry of the Ga-richest alloy, $\mathrm{AuGa_2}$. That is why the excess of released Ga appears as metallic with advancement of the reaction. The replacement of the interfacial Au film by an Au-gallide alloy leads to appreciable SBH reduction. As can be seen in Fig. 4 there is striking correlation between the enrichment of the Au-gallide alloy with Ga, reflected by the weight of the Ga(Au) component, and the SBH reduction. A simple phenomenological interpretation of the lowering of the SBH with increasing Ga content is contained in Eq. (1), replacing $\chi_{\mathrm{Au}} = 2.54$ with $\chi_{\mathrm{AuGa2}} = 2.0$. A better understanding of the dependence of the electronic properties on the composition of the interfacial alloy film requires thorough calculations considering different bonding configurations of Au and Ga at the interface.

Perhaps the most surprising result is the identical barrier heights, measured in different areas of the laterally heterogeneous interface developed after annealing to 820 °C. An explanation of this result is provided by inspection of the plots in Fig. 4(a). They reveal that the Au coverage varies in concert with the weight of the Ga(Au) component but in fact the

Au/Ga(Au) ratio changes negligibly. This indicates that the gallide alloy on the different grains (see Fig. 3) has very similar stoichiometry and only the thickness of the film changes laterally. This result confirms that above 500 °C the SBH value is controlled by the composition of the Au-gallide interfacial layer.

V. CONCLUSIONS

The dependence of the electronic properties of Au/GaN interface on film morphology, chemical reactions and spatial chemical heterogeneity has been investigated using SPEM. It has been found that the interface formed at room temperature is unstable and undergoes structural rearrangements after mild annealing. The onset of a chemical reaction above 500 °C leads to formation of an Au gallide film with composition determined by the reaction temperature. The temperature-induced structural rearrangements and the interfacial chemical reactions modify the Schottky barrier height. The stoichiometry of the Au-gallide interfacial layer plays a crucial role in determining the barrier height value. The present detailed characterization of the Au/GaN interface is intimately linked to understanding the complex processes controlling the interface morphology and chemistry of other similar Schottky contacts, where the metals (e.g., Pt,Pd,Ni) form gallides at elevated temperature.

ACKNOWLEDGMENTS

We are grateful to Professor R. Cingolani for stimulating this study and providing GaN samples, to Dr. M. Marsi and Dr. R. Cimino for a critical reading of the manuscript, and to D. Lonza for the valuable technical support. This work was supported by Sincrotrone Trieste under Grant No. EV 15.

[1] S. C. Jain, M. Willinder, J. Narayan, and R. van Overstraeten, J. Appl. Phys. **67**, 965 (2000).
[2] Q. Z. Liu and S. S. Lau, Solid-State Electron. **42**, 677 (1998).
[3] G. Popovici, H. Morkoc, and S. N. Mohammad, in *Group III Nitride Semiconductor Compounds*, edited by B. Gil (Clarendon, Oxford, 1998), pp. 19–69.
[4] Y. Kribes, I. Harrison, B. Tuck, T. S. Cheng, and C. T. Foxon, Semicond. Sci. Technol. **12**, 913 (1997), and references therein.
[5] R. Sporken, C. Silien, F. Malengreau, K. Grigorov, R. Caudano, F. J. Sanchez, E. Calleja, E. Munos, B. Beaumont, and P. Gibard, MRS Internet J. Nitride Semicond. Res. **2**, 23 (1997).
[6] L. He, X. J. Wang, and R. Zhang, J. Vac. Sci. Technol. A **17**, 1217 (1999).
[7] L. D. Bell, R. P. Smith, B. T. McDermott, E. R. Gertner, R. Pittman, R. L. Pierson, and G. L. Sullivan, Appl. Phys. Lett. **76**, 1725 (2000).
[8] C. I. Wu and A. Kahn, J. Vac. Sci. Technol. B **16**, 2218 (1998).
[9] S. Picozzi, A. Continenza, G. Satta, S. Massidda, and A. J. Freeman, Phys. Rev. B **61**, 16 736 (2000).
[10] M. Marsi *et al.*, J. Electron Spectrosc. Relat. Phenom. **84**, 73 (1997).
[11] L. Gregoratti, M. Marsi, and M. Kiskinova, Synchrotron Rad. News **12**, 40 (1999).
[12] V. M. Bermudez, D. D. Kolesce, and A. E. Wickenden, Appl. Surf. Sci. **126**, 69 (1998).
[13] A. R. Smith, R. M. Feenstra, D. W. Greve, J. Neugerbauer, and J. E. Northrup, Phys. Rev. Lett. **20**, 3934 (1997); **20**, 3934 (1997).
[14] M. Alonso, R. Cimino, and K. Horn, Phys. Rev. Lett. **64**, 1947 (1990).
[15] M. Marsi *et al.*, J. Electron Spectrosc. Relat. Phenom. **94**, 149 (1998).
[16] R. A. Beach, E. C. Piquette and T. C. McGill, MRS Internet J. Nitride Semicond. Res. **4S1**, G6.26 (1999).
[17] M-H. Kim, S-N. Lee, Ch. Huh, S. Y. Park, J. Y. Han, J. M. Seo, and S.-J. Park, Phys. Rev. B **61**, 10 966 (2000).
[18] S. M. Gasser, E. Kolawa, and M.-A. Nicolet, J. Vac. Sci. Technol. A **17**, 2642 (1999).
[19] A. Barinov, L. Casalis, L. Gregoratti, and M. Kiskinova, J. Phys. D **34**, 1 (2001).
[20] W. Mönch, J. Vac. Sci. Technol. B **17**, 1867 (1999), and references therein.
[21] W. Mönch, J. Appl. Phys. **80**, 5076 (1996).
[22] *Semiconductors—Basic Data*, edited by O. Madelung (Springer-Verlag, Berlin, 1996).
[23] V. M. Bermudez, J. Appl. Phys. **86**, 1170 (1999), and references therein.
[24] R. Schlaf, R. Hinogami, M. Fugitani, S. Jae, and Y. Nakato, J. Vac. Sci. Technol. A **17**, 164 (1999).
[25] J. A. Venables, G. H. T. Spiller, and M. Hanbücken, Rep. Prog. Phys. **47**, 399 (1984).
[26] M. Hansen, *Constitution of Binary Alloys*, Metallurgy and Metallurgical Engineering Series, edited by R. F. Mehl (McGraw-Hill, New York, 1958).